NJC

PAPER

View Article Online
View Journal | View Issue

Cite this: *New J. Chem.*, 2015, 39, 4047

AACVD of $Cu_{2-x}S$, In_2S_3 and $CuInS_2$ thin films from $[Cu(^iBu_2PS_2)(PPh_3)_2]$ and $[In(^iBu_2PS_2)_3]$ as single source precursors

Sajid N. Malik,[ab] Abdul Qadeer Malik,[b] Rana Farhat Mehmood,[c] Ghulam Murtaza,[a] Yousef G. Alghamdi[d] and Mohammad Azad Malik*[a]

Received (in Montpellier, France) 11th December 2014,
Accepted 10th March 2015

DOI: 10.1039/c4nj02289k

www.rsc.org/njc

$[In(^iBu_2PS_2)_3]$ and $[Cu(^iBu_2PS_2)(PPh_3)_2]$ complexes have been synthesized and used as single source precursors to deposit thin films of cubic In_2S_3 and $Cu_{2-x}S$ respectively on glass substrates by aerosol-assisted chemical vapor deposition (AACVD) at 350–500 °C. Thin films of $CuInS_2$ have also been deposited by using 1 : 1 molar ratio of $[In(^iBu_2PS_2)_3]$ and $[Cu(^iBu_2PS_2)(PPh_3)_2]$. The deposited thin films were characterized by X-ray diffraction (XRD), scanning electron microscopy (SEM) and energy dispersive X-ray diffraction (EDX) techniques. Deposition of films at different temperatures showed significant variation in stoichiometry and microstructure. The $CuInS_2$ thin films were ultrasonicated in toluene along with dodecanthiol for 3 hours to obtain a suspension of $CuInS_2$ nanocrystallites with a diameter of *ca.* 18 ± 2 nm and a band gap of 1.59 eV.

1. Introduction

Semiconductor nanoparticles and thin films of metal sulfides have attracted a great deal of research attention by theoretical and experimental chemists all over the world during the past few decades.[1] Exciting size dependent properties of these materials can be tailored for use in a wide range of applications.[2] Therefore, preparation of metal sulfide nanostructures with fine-tuned properties for specific applications has been a challenge for material chemists.

Copper sulfide thin films have been utilized as photo-absorber in CdS–Cu_xS solar cells in 1950.[3] However, renewed interest of the scientific community in copper sulfide chiefly emerged with the discovery of a range of distinct crystallographic phases and stoichiometric combinations of Cu_xS (where $1 < x > 2$). Other important features of copper sulfide include its lower toxicity as compared with other compound semiconductors and its earth abundant nature. Copper sulfide exhibits bulk band gap energies of ≥ 1.2 eV and has been used as a p-type semiconductor in many optoelectronic devices like solar cells, gas sensors,[4] optical filters, and electro-conductive electrodes.[5] Further applications of copper sulfide thin films include microwave shielding, photocatalysis,[6] cathode material in lithium batteries,[7] water splitting[8] and as solar control coatings.[9] Furthermore, it has also been investigated as an important bio-imaging,[10] photo-thermal therapeutic[11] and thermoelectric material.[12]

Indium sulfide, a wide band gap material of III–VI semiconductor family, has a band gap energy 2–2.3 eV and 2.8 eV. Owing to the stability, optical transparency, high photosensitivity, lower toxicity and photoconductive behaviour, indium sulfide thin films find their use in important technological applications like photocatalysis,[13] water splitting[14] and solar photovoltaics.[15] Solar cells based on β-In_2S_3 have already shown a power conversion efficiency of 16.4% which is more or less comparable to the CdS based solar devices. Therefore, indium sulfide is being considered as an alternative material to highly toxic CdS.[16]

Copper indium disulfide ($CuInS_2$) is an important ternary chalcogenide material of I–III–VI family of compound semiconductors. It has a direct band gap value of 1.5 eV which closely matches with the solar spectrum. Furthermore, $CuInS_2$ has an excellent photo-irradiation stability as well as a high absorption coefficient ($>10^5$). Therefore, $CuInS_2$ was investigated as the material of choice for thin film solar photovoltaics.[17] Solar cells based on its quaternary selenium analogue $CuIn_xGa_{1-x}Se_2$ have already demonstrated a sub-module power conversion efficiency of 20.4%.[18] Theoretical calculations suggest power conversion efficiencies of 27–32% for $CuInS_2$ based solar cells.[19] However, the practical efficiencies are limited to only 13% due to recombination

[a] *Schools of Chemistry and Materials, The University of Manchester, Oxford Road, Manchester, M13 9PL UK. E-mail: azad.malik@manchester.ac.uk; Fax: +44 (0)161-275-4616; Tel: +44 (0)161-275-465*
[b] *School of Chemical & Materials Engineering, National University of Sciences and Technology, Islamabad 44000, Pakistan*
[c] *Institute of Chemical Sciences, Bahauddin Zakariya University, Multan 60000, Pakistan*
[d] *Department of Chemistry, Faculty of Science & Art – Rabigh, King Abdulaziz University, Jeddah, Saudi Arabia*

losses in the space charge region.[20] $CuInS_2$ nanostructures also find other important applications like bio-imaging,[21] H_2 evolution from water,[22] light emitting diodes[23] and as a counter electrode material for dye sensitized solar cells.[24]

A variety of wet and dry methods have been used for deposition of metal sulfide thin films. These methods include chemical bath deposition,[25] spin coating,[26] chemical spray pyrolysis,[27] successive ion layer adsorption and reaction (SILAR),[28] physical vapor deposition (PVD),[29] atomic layer deposition (ALD),[30] modulated flux deposition,[31] electrodeposition[32] and metal–organic chemical vapor deposition (MOCVD)[33] including aerosol assisted chemical vapor deposition (AACVD).[34] It has been found that the thin films deposited by different techniques have different phase structure and degree of crystallinity, thus showing variable electrical as well as optoelectronic properties. Precise control over phase structure and stoichiometry of the deposited metal sulfides is still an important research challenge.

Chemical vapor deposition (CVD) offers good control over morphology, stoichiometry and phase structure of the deposited material. Furthermore, this technique has demonstrated an excellent potential for scaling up the film deposition process. Therefore, CVD routes have attracted remarkable research attention and resultantly there has been an ever increasing interest of the scientific community in the design of CVD precursors. In contrast to conventional CVD, AACVD technique circumvents the requirements of volatility and thermal stability of the precursors. Furthermore, judicious design of precursors coupled with careful control of deposition conditions like solvent, precursor concentration, carrier gas flux and deposition temperature can provide high quality thin films for technologically demanding applications. Therefore, our research efforts focus on exploring metal–organic compounds as molecular precursors for deposition of metal chalcogenide nanostructures and thin films.

Dialkyldithiophospinate compounds have, since long, been used as insecticides, additives to lubricants and flotation agent for metals on industrial scale.[35] Previously, we have synthesized diisobutyldithiophosphinato-complexes of Cd and Zn and used them as single-source precursor for deposition of CdS and ZnS thin films by LP-MOCVD.[36] We have also synthesized dialkyldiselenophosphinato-complexes of In(III) and Ga(III).[37] Herein, we report the deposition of thin films of copper sulfide, indium sulfide and their ternary analogue $CuInS_2$ from Ph_3P-stabilized diisobutyldithiophosphinato-copper(I) and tris(diisobutyldithiophosphinato)indium(III) complexes by AACVD technique.

2. Experimental

2.1 Chemicals used and the physical measurements

Sodium diisobutyldithiophosphinate (50% solution in water), copper(II) chloride and indium(III) chloride were purchased from Sigma-Aldrich and used as received. Precursor complexes $[In(^iBu_2PS_2)_3]$ (**1**) and $[Cu(^iBu_2PS_2)(PPh_3)_2]$ (**2**) were synthesized in accordance with the procedure already reported by Kuchen *et al.*[38] Solvents used in this work (methanol and toluene) were distilled over calcium hydride and sodium/benzophenone before each experiment. Bruker AC300 FT-NMR spectrometer was used to record ^1H NMR spectra whereas the mass spectra were recorded on a Kratos Concept 1S instrument. Microanalyses were carried out by the University of Manchester microanalysis facility using CHN Analyzer (LECO model CHNS-932). Melting points were recorded using a Stuart melting point apparatus and are uncorrected.

2.2 Synthesis of precursor complexes

2.2.1 $[In(^iBu_2PS_2)_3]$ (1). The indium complex (**1**) was synthesized by the reaction of sodium diisobutyldithiophosphinate and $InCl_3$ using literature procedure as reported by Kuchen *et al.*[38] The white precipitate obtained from reaction in aqueous medium was filtered under vacuum and recrystallized from toluene to give clear white crystals which were filtered under suction and dried in vacuum.

2.2.2 $[Cu(^iBu_2PS_2)(PPh_3)_2]$ (2). The copper complex (**2**) was prepared by the reaction of dry $Na^iBu_2PS_2$, CuCl and Ph_3P in CH_2Cl_2 as per already reported procedure.[39] The reaction products were filtered and concentrated. The concentrate was left for several days at room temperature and 'yielded complex (**2**) as white transparent plate like crystals.

2.3 Deposition of thin films by AACVD

The thin films were deposited onto glass slides of 1 × 3 cm dimensions. The substrates were subjected to rigorous cleaning to remove any contamination. An improvised AACVD kit described elsewhere was used for performing thin film deposition experiments.[40] Typical procedure for AACVD experiments involved dissolving 0.3 mmol of the precursor (or a mixture of 0.15 mmol $[In(^iBu_2PS_2)_3]$ and 0.15 mmol $[Cu(^iBu_2PS_2)(PPh_3)_2]$ in case of $CuInS_2$ thin films) in 15 mL toluene. The precursor solution was then loaded in a two-necked round-bottom flask (150 mL), one end of which was connected with the carrier gas (argon) inlet while the other end joined to the reactor tube by means of a reinforced tubing. Flow rate of the argon was maintained at 130 mL min^{-1} by using a Platon flow gauge. Aerosols of the precursor solution were generated by placing the round-bottom flask containing the precursor solution on a water bath above the piezoelectric modulator of a PIFCO ultrasonic humidifier. The stream of carrier gas transferred thus generated aerosols to the hot zone of the reactor placed in a Carbolite furnace and maintained at desired deposition temperature. Six glass substrates were placed in the reactor. Upon reaching the hot substrate surface, thermolysis of the solvent and the precursor occurs and thermally induced reactions lead to deposition of the thin films onto the substrate. Deposition experiments were performed at four different temperatures *i.e.*, 350, 400, 450 and 500 °C at a constant argon flow rate for ~1.5 h duration.

A Bruker D8 AXE diffractometer was used to record the p-XRD patterns of the thin films, which were scanned from 20 to 80 degrees with the step size of 0.02. Microstructural details and morphology of the thin films were examined using a Philips XL 30 FEGSEM scanning electron microscope. Carbon coating of the thin films was carried out using an Edwards

E-11306A coating system before SEM imaging. EDX analyses for determining elemental composition of the thin films were performed using a DX4 instrument.

3. Results and discussion

The precursor complex (**1**) showed excellent moisture and air stability for several months. However, complex (**2**) tends to decompose upon long term storage and was therefore stored under nitrogen. Both of the complexes were characterized by FTIR, NMR, APCI-MS spectrometry and elemental analysis. These complexes were then used as precursors for the deposition of $Cu_{2-x}S$, In_2S_3 and $CuInS_2$ thin films by AACVD.

3.1 Thermogravimetric analyses

Thermal decomposition profile of the complexes (**I**) and (**II**) was studied by the thermogravimetric analyses (TGA). TGA curves of the copper and indium complexes are shown in Fig. 1. The TGA curve of the indium complex (**1**) shows that its decomposition starts at 268 °C and completes in a single step at 396 °C leaving behind a 29.89% residue which closely matches with the calculated value for In_2S_3 (30.34%).

The TGA curve for the copper complex (**II**) shows that this complex also decomposes in a single step. The decomposition process starts at slightly higher temperature of 296 °C and completes at 371 °C leaving a 22.85% residue which is fairly close to the calculated value for Cu_2S (21.96%).

3.2 Deposition of copper sulfide thin films

Copper sulfide thin films were deposited by AACVD onto glass substrates from $[Cu(^{i}Bu_2PS_2)(PPh_3)_2]$ at temperatures ranging from 350 to 500 °C. Deposition experiment at 350 °C gave dull black films with a grey residue on the surface. Black thin layer was well adhered to the substrate, however the greyish surface material was removed during the scotch tape testing. At higher temperatures of 400 °C, 450 °C and 500 °C, bluish black films were deposited onto the substrate which successfully passed

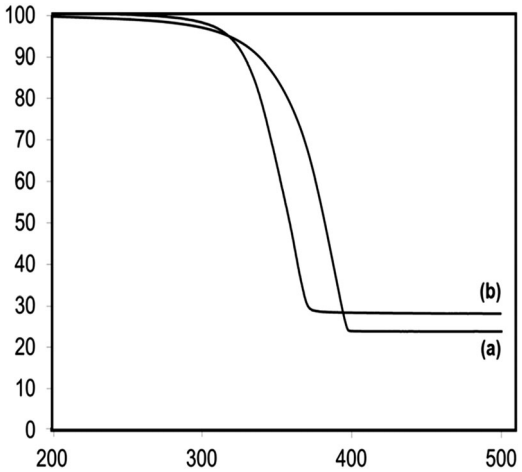

Fig. 1 TGA curves showing decomposition behaviour of (a) $[In(^{i}Bu_2PS_2)_3]$ and (b) $[Cu(^{i}Bu_2PS_2)(PPh_3)_2]$ complexes.

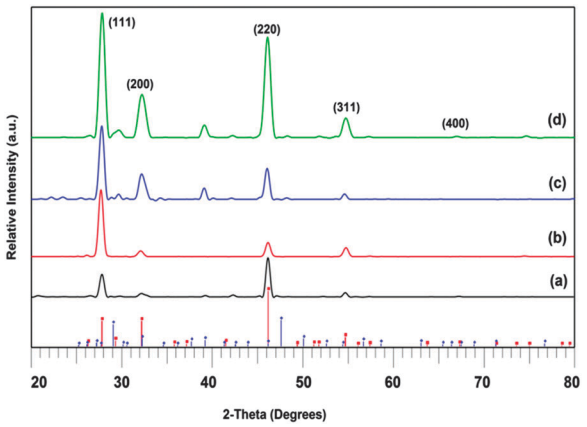

Fig. 2 The p-XRD patterns of $Cu_{2-x}S$ thin films deposited from $[Cu(^{i}Bu_2PS_2)(PPh_3)_2]$ at different temperatures (a) 350 °C, (b) 400 °C, (c) 450 °C and (d) 500 °C. Vertical lines below show the standard ICDD patterns 024-0061 (red) for cubic digenite and 00-047-1748 (blue) for rhombohedral digenite phase of $Cu_{2-x}S$.

the scotch tape test. Almost uniform coverage of the substrates was observed at all temperatures. The powder X-ray diffraction (p-XRD) patterns of thin films grown at 350, 400, 450 and 500 °C are shown in Fig. 2. The p-XRD patterns show deposition of a biphasic mixture of cubic digenite $Cu_{7.2}S_4$ (ICDD pattern 00-024-0061) and rhombohedral digenite Cu_9S_5 (ICDD pattern 00-047-1748) at 350 °C, 450 °C and 500 °C temperatures. However, AACVD experiment at 400 °C resulted in the deposition of pure monophasic material corresponding to the rhombohedral digenite Cu_9S_5. Relatively sharper peaks were observed for thin films deposited at 450 °C and 500 °C which might be attributed to improved crystallinity of the material deposited at higher temperatures.

The microstructure of as deposited $Cu_{2-x}S$ thin films was examined using scanning electron microscopy. SEM images of $Cu_{2-x}S$ films deposited at different temperatures are given in Fig. 3. The micrographs clearly show that morphology of the materials deposited at different temperatures is distinctively different. The SEM image of the thin films deposited at 350 °C showed a thick layer of poorly adsorbed material covering a very thin layer of small globular crystallites. Randomly oriented crystallites with multiple facets were observed in the films deposited at 400 °C. Thin film deposited at 450 °C demonstrated growth of similar grains with a small fraction of loose grey material. The SEM image for thin film deposited at 500 °C shows predominant growth of large rhombohedral and triangular crystallites. The crystallites deposited at 500 °C had a size of about 1.0–1.2 μm, whereas thin films deposited at 400 and 450 °C comprised of submicron sized crystallites. Results of the EDX analysis for thin films deposited on various temperatures are summarized in Table 1. Deviation from normal stoichiometric ratio of 2 : 1 for copper and sulfur was observed in EDX analyses. Furthermore, variation in stoichiometric composition of individual grains was also indicated by EDX analyses.

Optical band gap of the film deposited at 450 °C was determined by extrapolating the linear portion of the $(\alpha h\nu)^2$ *vs.* $h\nu$ curve

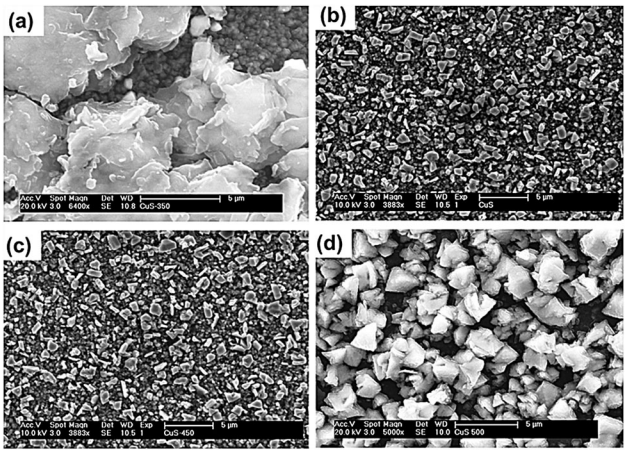

Fig. 3 SEM images of as deposited thin films of $Cu_{2-x}S$ at (a) 350 °C (b) 400 °C and (c) 450 °C and (d) 500 °C.

Table 1 EDX analyses results of thin films deposited at different temperatures

Material	Deposition temperature (°C)	EDX analyses results atomic percentage (%) Cu	In	S	P
$Cu_{2-x}S$, digenite	350	61.9377	—	38.0623	
00-024-0061	400	62.8425	—	37.1575	
00-047-1748	450	62.1039	—	37.8961	
	500	63.3231	—	36.6769	
In_2S_3, cubic	350	—	41.3432	58.6568	
01-084-1385	400	—	42.4768	57.5232	
	450	—	41.9436	58.0564	
	500	—	43.0286	56.9714	
$CuInS_2$, roquesite	350	24.9663	25.6206	46.4954	2.9177
00-027-0159	400	26.1627	26.5356	47.3017	
	450	26.2351	26.4152	47.3497	
	500	26.2051	26.4460	47.3489	

to the $h\nu$ axis, where $(\alpha h\nu)^2 = 0$, and was found to be ~1.82 eV. The reported band gap values for copper sulfide thin films vary from 1.67 eV to 1.99 eV depending upon the technique used for deposition of thin films.[11]

3.3 Deposition of indium sulfide thin films

In_2S_3 thin films were deposited onto glass substrates from $[In(^iBu_2PS_2)_3]$ by AACVD at 350 °C to 500 °C. A brownish red indium sulfide thin film was deposited at all temperatures. The as-deposited In_2S_3 thin films were well adhered to the substrate and successfully qualified the scotch tape test. p-XRD patterns of the In_2S_3 thin films deposited at different temperatures are given in Fig. 4. The p-XRD patterns demonstrate the deposition of monophasic In_2S_3 at all the deposition temperatures. This phase of In_2S_3 corresponds to the standard ICDD pattern 01-084-1385 for cubic In_2S_3 having a space group $Fd\bar{3}m$. The p-XRD peaks for thin films grown at higher temperature become narrower and sharper which may be attributed to more pronounced growth and improved crystallinity of the grains in the deposited material.

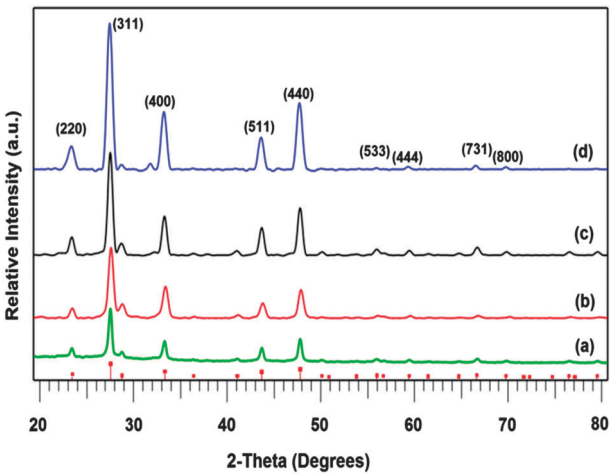

Fig. 4 p-XRD patterns of as deposited In_2S_3 thin films from $In[(^iBu_2PS_2)_3]$ precursor at temperatures (a) 350 °C, (b) 400 °C, (c) 450 °C and (d) 500 °C. Vertical lines below show the standard ICDD pattern 01-084-1385 for In_2S_3.

Surface morphology and microstructure of the as-deposited In_2S_3 thin films were studied using SEM imaging. The SEM images reveal homogenous coverage of substrates by the deposited material at all the deposition temperatures. However, remarkable differences in morphology of the deposited material were evident in the SEM images of films deposited at different temperatures (Fig. 5).

The In_2S_3 films deposited at 350 and 400 °C consist of very small grains of undefined shape with no distinguishable grain boundaries. Thin film deposited at 450 °C showed cubic and rectangular grains evolving from smaller crystallites. Highly crystalline grains of cubic structure and well defined grain boundaries were observed in the film deposited at 500 °C. Such films with smooth and uniform coverage, controlled morphology and good crystallinity might offer fairly good power conversion efficiencies in solar photovoltaic devices. EDX analysis of the as-deposited thin films showed no appreciable

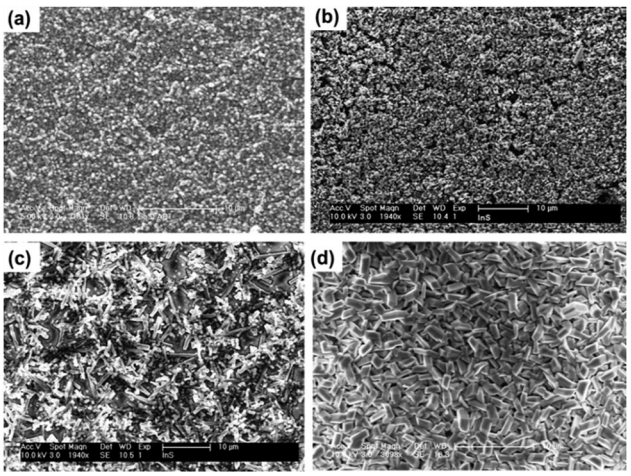

Fig. 5 SEM images of as deposited In_2S_3 thin films at (a) 350 °C (b) 400 °C (c) 450 °C and (d) 500 °C.

differences in the stoichiometric composition of the material deposited at various deposition temperatures. Furthermore, no remarkable variation in composition of the individual grains could be determined within the analytical limits of EDX technique. Band gap energy calculated for In_2S_3 thin film deposited at 450 °C was found to be 2.15 eV. Literature values for band gap of indium sulfide thin films are 2.0 to 2.4 eV and 2.8 eV depending on their synthesis process and on their composition.[41]

3.4 Deposition of $CuInS_2$ thin films

$CuInS_2$ thin films were deposited using equimolar mixture of complex (**1**) and (**2**) in toluene during AACVD experiment. The deposition at 350 °C yielded a poorly covered film. However, the depositions at higher temperatures *i.e.* 400 °C to 500 °C yielded greyish black, uniform films.

The crystallographic phase of the deposited material was determined by the p-XRD studies. The powder X-ray diffraction patterns of the thin films deposited at various temperatures are shown in Fig. 6. The p-XRD studies demonstrated that the tetragonal phase of $CuInS_2$ (standard ICDD pattern 00-027-0159) had been deposited at all the deposition temperatures with the material having a preferred orientation along (112) plane. This is typical for ternary copper chalcopyrite compounds deposited by CVD. Broader peaks for the material deposited at 350 °C reflect smaller size and poor crystallinity of thin films deposited at 350 °C. However, relatively sharp peaks were observed in the p-XRD pattern of thin films deposited at higher temperatures. No additional peaks from binary copper and/or indium sulfide materials were observed.

The SEM images (Fig. 7) show that the films deposited at different temperatures have a remarkably different microstructure. As indicated by the p-XRD studies, the films deposited at 350 °C consist of very small crystallites with the surface covered by loosely bound material of undefined shape.

Small flakes forming flower like clusters were observed in the film deposited at 400 °C. The material deposited at 450 °C comprised of randomly oriented flake like structures having a length of ~10 μm and a diameter of *ca.* 0.8 μm, uniformly covering the substrate. A more pronounced growth in these flake like structures was observed in the thin film deposited at 500 °C where the flakes have a length ranging from 25–35 μm. EDX analysis (Table 1) confirmed that the deposited material had a stoichiometric ratio of 1:1:2 for Cu, In and S respectively. Elemental mapping (Fig. 7e) confirmed the uniform distribution of the Cu, In and S throughout the film. Furthermore, no notable differences in the stoichiometry of the individual grains could be observed. A small contamination of phosphorus (<3%) was found on the film deposited at 350 °C. No such contamination can be observed on the films deposited at higher temperatures.

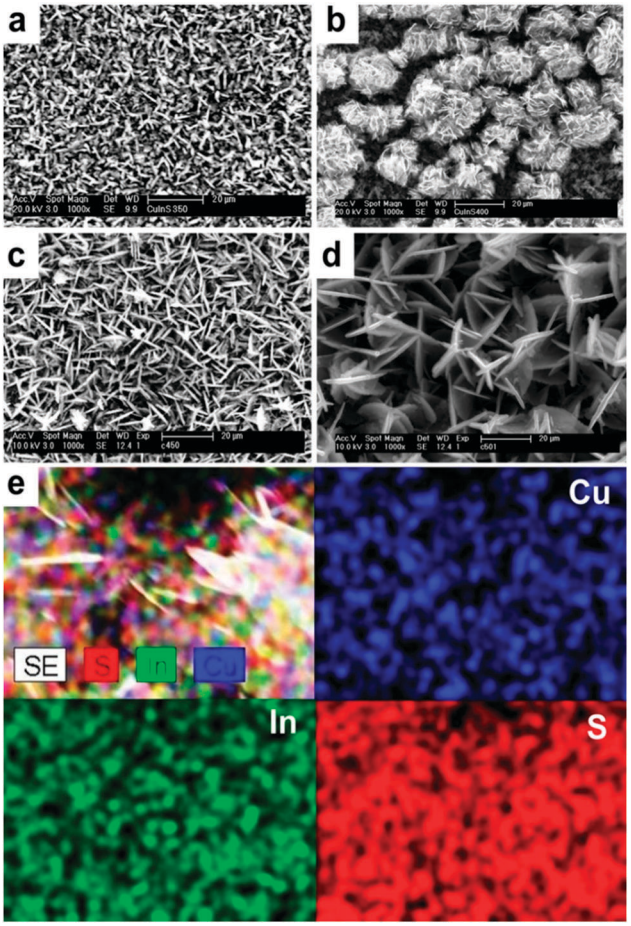

Fig. 7 SEM images of as deposited thin films of $CuInS_2$ at (a) 350 °C, (b) 400 °C, (c) 450 °C (d) 500 °C (e) EDX elemental map showing uniform distribution of Cu, In and S in $CuInS_2$ thin film.

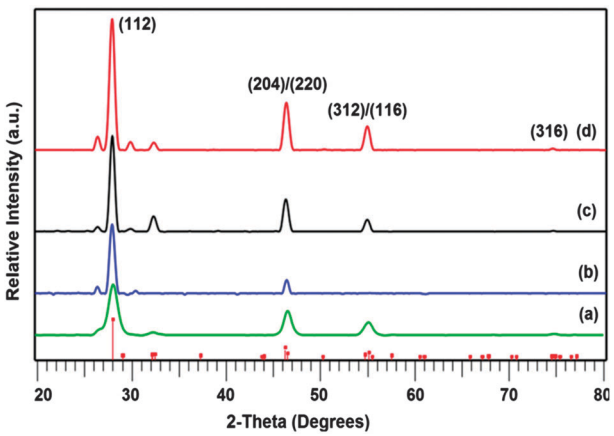

Fig. 6 p-XRD patterns of as deposited $CuInS_2$ thin films from 1:1 molar ratios of copper and indium precursor at temperatures (a) 350 °C, (b) 400 °C, (c) 450 °C and (d) 500 °C indexed with standard ICDD pattern 00-027-0159.

The deposition of $CuInS_2$ thin films by CVD using molecular precursors has been reported by Nomura *et al.* using $[Bu_2In(S^iPr)Cu(S_2CN^iPr_2)]$ as a single source precursor.[42] The p-XRD studies showed the deposition of polyphasic mixtures of either $CuInS_2$ and $CuIn_5S_8$ or $CuInS_2$ and In_6S_7 phases. Hepp and co-workers synthesized a number of complexes as single-source precursors for deposition of ternary copper chalcogenide thin films.[43] O'Brien *et al.* have also reported the deposition of $CuInS_2$ thin films by using asymmetrical dialkyldithiocarbamate

complexes as molecular precursors.[44] They have also synthesized $[(Ph_3P)Cu(SC\{O\}Ph)_3In(SC\{O\}Ph)]$ complex as single source precursor for $CuInS_2$.[45] However, AACVD using this precursor resulted into deposition of β-In_2S_3 rather than $CuInS_2$. Similarly, Shim and co-workers have deposited $CuInS_2$ thin films by MOCVD using bis(ethylisobutylacetato)copper(II) and tris(*N*,*N*-ethylbutyldithiocarbamato)indium(III) precursors.[46]

Most of these reports either involve a precursor which is difficult to synthesise or the deposited materials were a mixture of binary and ternary phases. Furthermore, deposition of $CuInS_2$ thin films sometimes involves an intricate two-stage deposition methodology whereby copper film is deposited first, followed by deposition of indium sulfide and subsequent reaction of binary phases to form ternary $CuInS_2$, as in case of Shim *et al.*[46] The current work presents a simple, straightforward, non-vacuum and scalable method for the deposition of good quality, phase pure $CuInS_2$ thin films at moderate temperatures from easily synthesized, air stable and environmentally benign molecular complexes. Post deposition treatments like annealing may further improve the microstructure, crystallinity as well as overall quality of as deposited thin films, as reported by Kelly and co-workers.[47]

3.5 Sonochemical preparation of $CuInS_2$ nanoink

$CuInS_2$ thin films deposited at 450 °C along with 5 mL dodecanthiol were sonicated in toluene for 3 hours to yield nanoparticles which were dispersible in toluene and hexane.

The nanoparticles thus obtained were washed thrice with ethanol through centrifugation to remove extra dodecanthiol and dispersed in toluene. No agglomeration was observed in the nanoparticles upon storage for 1 week. p-XRD studies revealed that the diffraction pattern (Fig. 8a) recorded for thus obtained nanoparticles corresponds to the tetragonal $CuInS_2$ (standard ICDD pattern 00-027-0159) having $I\bar{4}2d$ space group.

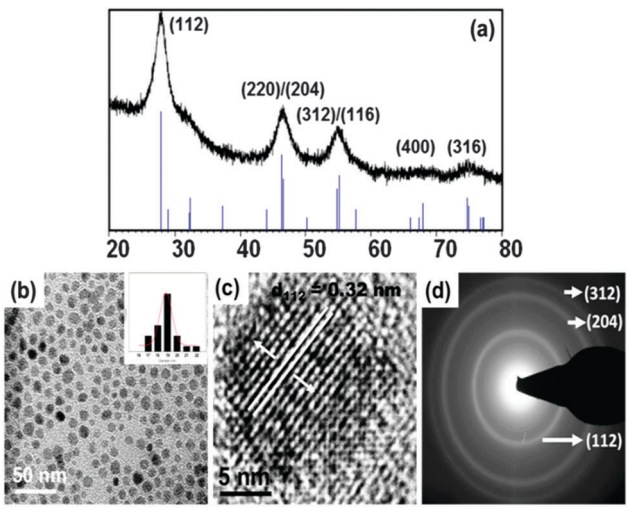

Fig. 8 (a) p-XRD (b) TEM (c) HR-TEM and (d) SAED pattern of as prepared $CuInS_2$ nanoink. Figure in inset shows the size distribution histogram of $CuInS_2$ nanoparticles.

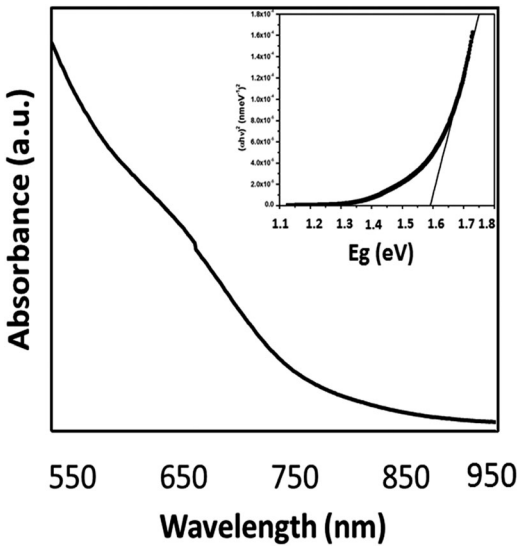

Fig. 9 UV-vis-NIR absorption spectrum of $CuInS_2$ (in toluene) suspension of nanoparticles. Figure in inset shows the band gap of 1.59 eV for $CuInS_2$ nanoink.

Scherrer formula was used to calculate the mean diameter of the crystallites which was found to be 18.2 nm.

The TEM images recorded for as obtained nano-ink are shown in Fig. 8b. TEM microscopy revealed formation of well dispersed quasi-spherical nanoparticles with very little/no agglomeration. The mean diameter of the nanoparticles calculated from TEM image using image analysis software (ImageJ) was found to be 19 ± 2.2 nm which was in fair agreement with the result obtained from Scherrer equation (*ca.* 18.2 nm). HR-TEM image (Fig. 8c) clearly showed the lattice fringes and inter-planer distance was calculated to be 0.32 nm which corresponds to the *d*-spacing of the (112) plane of the tetragonal $CuInS_2$ material. Selected area electron diffraction (SAED) pattern (Fig. 8d) indicates that the nanoparticles are polycrystalline in nature and showed three concentric diffraction rings corresponding to (112), (204) and (312) planes of the $CuInS_2$ lattice. Nanoparticles thus obtained showed a band gap of 1.59 eV (Fig. 9) which is slightly higher than that for the bulk $CuInS_2$ material. This may be attributed to nano-size domain of the crystallites obtained in this work.

4. Conclusions

Good quality thin films of $Cu_{2-x}S$, In_2S_3 and $CuInS_2$ were deposited by aerosol assisted chemical vapor deposition (AACVD) method using $[Cu(^iBu_2PS_2)(PPh_3)_2]$ and $[In(^iBu_2PS_2)_3]$ complexes as precursors. Deposition from $[Cu(^iBu_2PS_2)(PPh_3)_2]$ produced a mixture of cubic and rhombohedral digenite $Cu_{2-x}S$ at 350 °C, 450 °C and 500 °C and monophasic rhombohedral digenite $Cu_{2-x}S$ at 400 °C. Films grown from $[In(^iBu_2PS_2)_3]$ gave monophasic cubic In_2S_3 whereas 1 : 1 molar mixture of $[Cu(^iBu_2PS_2)(PPh_3)_2]$ and $[In(^iBu_2PS_2)_3]$ yielded tetragonal $CuInS_2$ thin films. Scanning electron microscopy (SEM) showed that the morphology and the microstructure of as deposited thin films significantly varies with the deposition

temperature in all the cases. While the deposited $Cu_{2-x}S$ thin films were not uniform, as deposited In_2S_3 and $CuInS_2$ thin films showed even coverage over the entire substrate as well as good crystallinity and may therefore be employed as photo-absorber in solar devices. Scratched $CuInS_2$ thin films, upon ultra-sonication, yielded $CuInS_2$ nanocrystals showing a diameter of 19 ± 2.2 nm. The work reported herein thus presents a simple and cost effective route for the deposition of copper based thin films. Detailed investigation into the efficiency of these materials for solar cell applications has yet to be carried out but is beyond the scope of this work.

Notes and references

1 K. Zare, M. Daroule, F. Mollaamine and M. Monajjemi, *Int. J. Phys. Sci.*, 2011, **6**, 2536; M. Monajjemi, L. Mahdavian, F. Mollaamin and K. Khaleghian, *J. Inorg. Chem.*, 2009, **54**, 1465; N. Revaprasadu, M. A. Malik and P. O'Brien, *J. Mater. Res.*, 1999, **14**, 3237; M. A. Malik, M. Motevalli and P. O'Brien, *Inorg. Chem.*, 1995, **34**, 6223; M. A. Malik, M. Motevalli, P. O'Brien and J. R. Walsh, *Organometallics*, 1992, **11**, 3136; A. A. M. Memon, M. Afzaal, M. A. Malik, C. Nguyen, P. O'Brien and J. Raftery, *Dalton Trans.*, 2006, 4499; D. J. Binks, S. P. Bants, D. P. West, M. A. Malik and P. O'Brien, *J. Mod. Opt.*, 2003, **50**, 299; C. Q. Nguyen, A. Adeogun, M. Afzaal, M. A. Malik and P. O'Brien, *Chem. Commun.*, 2006, 2182; M. A. Malik, M. Motevalli, T. Saeed and P. O'Brien, *Adv. Mater.*, 1993, **5**, 653; A. Panneerselvam, C. Q. Nguyen, M. A. Malik, P. O'Brien and J. Raftery, *J. Mater. Chem.*, 2009, **19**, 419–427.
2 Y. G. Sun and Y. N. Xia, *Science*, 2002, **298**, 2176.
3 D. C. Reynolds, G. Leies, L. T. Antes and R. E. Marburger, *Phys. Rev.*, 1954, **96**, 533.
4 A. Sagade, R. Sharma, R. S. Mane and S.-H. Han, *Sens. Transducers J.*, 2008, **95**, 81.
5 N. Farhadyar, M. S. Sadjadi, F. Farhadyar and A. Farhadyar, *J. Nano Res.*, 2013, **21**, 51.
6 B. Zeng, X. H. Chen, C. S. Chen, X. T. Ning and W. N. Deng, *J. Alloys Compd.*, 2014, **582**, 774.
7 B. Jache, B. Mogwitz, F. Klein and P. Adelhelm, *J. Power Sources*, 2014, **247**, 703; B. Zhang, X. W. Gao, J. Z. Wang, S. L. Chou, K. Konstantinov and H. K. Liu, *J. Nanosci. Nanotechnol.*, 2013, **13**, 1309.
8 Y. Im, S. Kang, K. M. Kim, T. Ju, G. B. Han, N. K. Park, T. J. Lee and M. Kang, *Int. J. Photoenergy*, 2013, **2013**, 452542.
9 S. Eda, K. Moriyasu, M. Fujishima, S. Nomura and H. Tada, *RSC Adv.*, 2013, **3**, 10414; P. K. Nair, V. M. Garcia, A. M. Ferndndez, H. S. Ruiz and M. T. S. Nair, *J. Phys. D: Appl. Phys.*, 1991, **24**, 441.
10 Y. D. Zhu, J. Peng, L. P. Jiang and J. J. Zhu, *Analyst*, 2014, **139**, 649; U. T. D. Thuy, N. Q. Liem, C. M. A. Parlett, G. M. Lalev and K. Wilson, *Catal. Commun.*, 2014, **44**, 62.
11 Z. B. Zha, S. M. Wang, S. H. Zhang, E. Z. Qu, H. T. Ke, J. R. Wang and Z. F. Dai, *Nanoscale*, 2013, **5**, 3216.
12 S. H. Chaki, M. P. Deshpande and J. P. Tailor, *Thin Solid Films*, 2014, **550**, 291.
13 R. Lucena, F. Fresno and J. C. Conesa, *Catal. Commun.*, 2012, **20**, 1.
14 D. Wei, Z. G. Lin, Z. T. Cui, S. Y. Su, D. K. Zhang, M. H. Cao and C. W. Hu, *Chem. Commun.*, 2013, **49**, 9609.
15 M. R. R. Menon, M. V. Maheshkumar, K. Sreekumar, C. S. Kartha and K. P. Vijayakumar, *Phys. Status Solidi A*, 2012, **209**, 199.
16 N. Naghavi, E. Chassaing, M. Bouttemy, G. Rocha, G. Renou, E. Leite, A. Etcheberry and D. Lincot, *European Materials Research Society Conference Symposium: Advanced Inorganic Materials and Concepts for Photovoltaics*, 2011, vol. 10; M. I. Hossain, P. Chelvanathan, M. Zaman, M. R. Karim, M. A. Alghoul and N. Amin, *Chalcogenide Lett.*, 2011, **8**, 315.
17 Z. Q. Yan, Y. Zhao, M. X. Zhuang, J. Liu and A. X. Wei, *J. Mater. Sci.: Mater. Electron.*, 2013, **24**, 5055.
18 P. Jackson, D. Hariskos, E. Lotter, S. Paetel, R. Wuerz, R. Menner, W. Wischmann and M. Powalla, *Prog. Photovoltaics*, 2011, **19**, 894.
19 S. T. Connor, C. M. Hsu, B. D. Weil, S. Aloni and Y. Cui, *J. Am. Chem. Soc.*, 2009, **131**, 4962.
20 S. Siebentritt, *Sol. Energy Mater. Sol. Cells*, 2011, **95**, 1471; H. Z. Zhong, Y. Zhou, M. F. Ye, Y. J. He, J. P. Ye, C. He, C. H. Yang and Y. F. Li, *Chem. Mater.*, 2008, **20**, 6434.
21 L. W. Liu, R. Hu, W. C. Law, I. Roy, J. Zhu, L. Ye, S. Y. Hu, X. H. Zhang and K. T. Yong, *Analyst*, 2013, **138**, 6144; K. Yu, P. Ng, J. Y. Ouyang, M. B. Zaman, A. Abulrob, T. N. Baral, D. Fatehi, Z. J. Jakubek, D. Kingston, X. H. Wu, X. Y. Liu, C. Hebert, D. M. Leek and D. M. Whitfield, *ACS Appl. Mater. Interfaces*, 2013, **5**, 2870.
22 I. Tsuji, H. Kato and A. Kudo, *Chem. Mater.*, 2006, **18**, 1969.
23 B. K. Chen, H. Z. Zhong, M. X. Wang, R. B. Liu and B. S. Zou, *Nanoscale*, 2013, **5**, 3514; H. Kim, J. Y. Han, D. S. Kang, S. W. Kim, D. S. Jang, M. Suh, A. Kirakosyan and D. Y. Jeon, *J. Cryst. Growth*, 2011, **326**, 90.
24 R. Y. Yao, Z. J. Zhou, Z. L. Hou, X. Wang, W. H. Zhou and S. X. Wu, *ACS Appl. Mater. Interfaces*, 2013, **5**, 3143.
25 J. S. Cruz, S. A. M. Hernandez, J. J. C. Hernandez, R. M. Rodriguez, R. C. Perez, G. T. Delgado and S. J. Sandoval, *Chalcogenide Lett.*, 2012, **9**, 85; B. Yahmadi, N. Kamoun, C. Guasch and R. Bennaceur, *Mater. Chem. Phys.*, 2011, **127**, 239; F. M. Cui, L. Wang, Z. Q. Xi, Y. Sun and D. R. Yang, *J. Mater. Sci.: Mater. Electron.*, 2009, **20**, 609.
26 Z. J. Zhou, J. Q. Fan, X. Wang, W. Z. Sun, W. H. Zhou, Z. L. Du and S. X. Wu, *ACS Appl. Mater. Interfaces*, 2011, **3**, 2189.
27 M. Rafi, Y. Arba, B. Hartiti, A. Ridah and P. Thevenin, *J. Optoelectron. Adv. Mater.*, 2013, **15**, 1328; P. V. Nho, P. H. Ngan, N. Q. Tien and H. D. Viet, *Chalcogenide Lett.*, 2012, **9**, 397; K. Otto, A. Katerski, A. Mere, O. Volobujeva and M. Krunks, *Thin Solid Films*, 2011, **519**, 3055.
28 H. M. Pathan, C. D. Lokhande, S. S. Kulkarni, D. P. Amalnerkar, T. Seth and S. H. Han, *Mater. Res. Bull.*, 2005, **40**, 1018; B. Maheswari and M. Dhanam, *Mater. Sci.*, 2013, **31**, 193; S. Lindroos, A. Arnold and M. Leskela, *Appl. Surf. Sci.*, 2000, **158**, 75.

29 C. Broussillou, M. Andrieux, M. Herbst-Ghysel, M. Jeandin, J. S. Jaime-Ferrer, S. Bodnar and E. Morin, *Sol. Energy Mater. Sol. Cells*, 2011, **95**, S13–S17; S. Gall, N. Barreau, S. Harel, J. C. Bernede and J. Kessler, *Thin Solid Films*, 2005, **480**, 138.

30 S. X. Lin, X. Z. Shi, X. Zhang, H. H. Kou and C. M. Wang, *Appl. Surf. Sci.*, 2010, **256**, 4365; J. Johansson, J. Kostamo, M. Karppinen and L. Niinisto, *J. Mater. Chem.*, 2002, **12**, 1022.

31 C. Guillen and J. Herrero, *Phys. Status Solidi A*, 2006, **203**, 2438.

32 J. L. Yuan, C. Shao, L. Zheng, M. M. Fan, H. Lu, C. J. Hao and D. L. Tao, *Vacuum*, 2014, **99**, 196; S. S. Dhasade, J. S. Patil, J. H. Kim, S. H. Han, M. C. Rath and V. J. Fulari, *Mater. Chem. Phys.*, 2012, **137**, 353.

33 S. S. Lee, K. W. Seo, J. P. Park, S. K. Kim and I. W. Shim, *Inorg. Chem.*, 2007, **46**, 1013; M. Kemmler, M. Lazell, P. O'Brien, D. J. Otway, J. H. Park and J. R. Walsh, *J. Mater. Sci.: Mater. Electron.*, 2002, **13**, 531.

34 M. A. Ehsan, T. A. N. Peiris, K. G. U. Wijayantha, M. M. Olmstead, Z. Arifin, M. Mazhar, K. M. Lo and V. McKee, *Dalton Trans.*, 2013, **42**, 10919; T. C. Deivaraj, J. H. Park, M. Afzaal, P. O'Brien and J. J. Vittal, *Chem. Mater.*, 2003, **15**, 2383; S. Saeed, N. Rashid, R. Hussain, M. A. Malik, P. O'Brien and W. T. Wong, *New J. Chem.*, 2013, **37**, 3214; A. L. Abdelhady, K. Ramasamy, M. A. Malik, P. O'Brien, S. J. Haigh and J. Raftery, *J. Mater. Chem.*, 2011, **21**, 17888.

35 W. Rickelton and R. Boyle, *Solvent Extr. Ion Exch.*, 1990, **8**, 783; I. Haiduc, D. Bryan-Sowerby and L. Shao-Fang, *Polyhedron*, 1995, **14**, 3389.

36 C. Byrom, M. A. Malik, P. O'Brien, A. J. P. White and D. J. Williams, *Polyhedron*, 2000, **19**, 211.

37 J. H. Park, P. O'Brien, A. J. P. White and D. J. Williams, *Inorg. Chem.*, 2001, **40**, 3629.

38 W. Kuchen, J. Metten and A. Judat, *Chem. Ber.*, 1964, **97**, 2306.

39 M. A. Malik, C. Byrom, P. O'Brien and M. Motevalli, *Inorg. Chim. Acta*, 2002, **338**, 245.

40 S. Mahboob, S. N. Malik, N. Haider, M. A. Malik and P. O'Brien, *J. Cryst. Growth*, 2014, **394**, 39.

41 N. Barreau, S. Marsillac, J. C. Bernede, T. Ben Nasrallah and S. Belgacem, *Phys. Status Solidi A*, 2001, **184**, 179.

42 R. Nomura, Y. Sekl and H. Matsuda, *J. Mater. Chem.*, 1992, **2**, 765–766.

43 J. A. Hollingsworth, A. F. Hepp and W. E. Buhro, *Chem. Vap. Deposition*, 1999, **5**, 105; K. K. Banger, J. Cowen and A. F. Hepp, *Chem. Mater.*, 2001, **13**, 3827; K. K. Banger, J. D. Harris, J. E. Cowen and A. F. Hepp, *Thin Solid Films*, 2002, **403**, 390–395; J. A. Hollingsworth, K. K. Banger, M. H. C. Jin, J. D. Harris, J. E. Cowen, E. W. Bohannan, J. A. Switzer, W. Buhro and A. F. Hepp, *Thin Solid Films*, 2003, **431**, 63–67; K. K. Banger, M. H. C. Jin, J. D. Harris, P. E. Fanwick and A. F. Hepp, *Inorg. Chem.*, 2003, **42**, 7713–7715.

44 M. Afzaal, D. Crouch, P. O'Brien and J. H. Park, *Progress in Semiconductor Materials for Optoelectronic Applications*, 2002, **692**, 215–220.

45 T. C. Deivaraj, J. H. Park, M. Afzaal, P. O'Brien and J. J. Vittal, *Chem. Mater.*, 2003, **15**, 2383–2391.

46 S. S. Lee, K. W. Seo, J. P. Park, S. K. Kim and I. W. Shim, *Inorg. Chem.*, 2007, **46**, 1013–1017.

47 C. V. Kelly, M. H. C. Jin, K. K. Banger, J. S. McNatt, J. E. Dickman and A. F. Hepp, *Mater. Sci. Eng., B*, 2005, **116**, 403–408.

